

Optimal transport of ultracold atoms in the non-adiabatic regime

A. COUVERT¹, T. KAWALEC¹, G. REINAUDI¹ and D. GUÉRY-ODELIN^{1,2(a)}

¹ *Laboratoire Kastler Brossel, CNRS UMR 8852, Ecole Normale Supérieure - 24 rue Lhomond, 75005 Paris, France, EU*

² *Laboratoire Collisions Agrégats Réactivité, CNRS UMR 5589, IRSAMC, Université Paul Sabatier 118 Route de Narbonne, 31062 Toulouse CEDEX 4, France, EU*

received 16 April 2008; accepted in final form 16 May 2008

published online 11 June 2008

PACS 37.10.Vz – Mechanical effects of light on atoms, molecules, and ions

PACS 37.10.Gh – Atom traps and guides

PACS 37.90.+j – Other topics in mechanical control of atoms, molecules, and ions

Abstract – We report the transport of ultracold atoms with optical tweezers in the non-adiabatic regime, *i.e.* on a time scale on the order of the oscillation period. We have found a set of discrete transport durations for which the transport is not accompanied by any excitation of the centre of mass of the cloud after the transport. We show that the residual amplitude of oscillation of the dipole mode is given by the Fourier transform of the velocity profile imposed to the trap for the transport. This formalism leads to a simple interpretation of our data and simple methods for optimizing trapped particles displacement in the non-adiabatic regime.

Copyright © EPLA, 2008

The controlled transport of ultracold atoms is crucial for the development of experiments in atomic physics. It makes possible the delivery of cold atoms in a region free of the laser beams and coils of the magneto-optical trap (MOT), allowing a better optical and mechanical access. It also opens new perspectives for probing a surface or any material structure, and for loading atoms in optical lattices, or for positioning atoms in a high- Q optical cavity [1,2]. In addition it opens the way to a new generation of experimental setups where ultracold clouds of atoms would be delivered on demand on a variety of different experimental platforms separated by macroscopic distances. This is standard for charged particles and energetic neutral particles, while it has only been recently accomplished with ultracold atoms by moving slowly optical tweezers [3]. Transport of cold packets of atoms is also of importance as a step towards the continuous production of a Bose-Einstein condensate [4,5].

Macroscopic transport of cold atoms has been demonstrated using several different configurations. One can move mechanically a pair of coils [6,7] or use a set of coils with time-varying currents [8]. Such quadrupolar traps are non-harmonic. Alternatively one can use traps with a harmonic shape near their bottom, such as Ioffe-Pritchard traps [5,9–11], optical tweezers as recently demonstrated

on Bose-condensed clouds [4] or 1D optical lattices [12,13]. The harmonic potential is of particular interest since the centre-of-mass motion (also referred to as Kohn's mode) is not coupled to the other degrees of freedom, and this is true both in the presence and in the absence of interactions between atoms and both for classical and quantum physics. However all these studies have been performed in the adiabatic regime where the duration of the transport is long with respect to the typical oscillation period of the trapped atoms. This is because a lot of energy is given to the trapped cloud when it is transported in the non-adiabatic regime, giving rise to heating and to a strong excitation of the dipole mode. This, in turn, can result in atom losses due to the finite depth of the trap. While microtraps can have high-oscillation frequencies, the traps allowing to transport a large number of atoms are not very steep and thus an adiabatic transport is quite long, limiting the repetition rate of the experiments performed. To our knowledge, the issue of an optimal transport beyond this limit has only been addressed numerically for ions in Paul traps [14].

In this letter we report the transport of a cold atom cloud in the non-adiabatic regime with a high degree of control by means of optical tweezers with no residual excitation of the dipole mode of oscillation, moderate heating and no losses. We also provide a simple theoretical model which permits to work out a new picture of the

^(a)E-mail: dgo@lkb.ens.fr

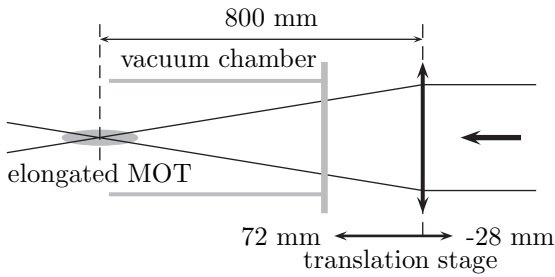


Fig. 1: Sketch of the main part of the experimental setup (not to scale) —see text.

transport. The residual amplitude of oscillation of the cloud can be expressed as the Fourier transform of the velocity profile imposed to the trap, yielding a simple interpretation of our data and providing simple methods for optimizing trapped particles displacement.

Our optical tweezers are generated by an ytterbium fibre laser (IPG LASER, model YLR-300-LP) with a central wavelength of 1072 nm. The wavelength of the laser is larger than the atomic resonance wavelengths of 780.24 nm and 794.98 nm of the rubidium 87 atoms, and thus, atoms are attracted to the region of maximum intensity [15]. The beam is focused inside the vacuum chamber by a lens with a 802 mm focal length mounted on a translation stage (Newport linear motor stage, model XMS100), allowing one to move the optical tweezers longitudinally on a 100 mm range with an absolute repeatability on the order of a few hundreds of nm (see fig. 1). The resulting waist has been measured to be $44 \mu\text{m}$, corresponding to a Rayleigh length of 5.7 mm.

The optical tweezers are loaded from an elongated MOT. The cigar shape of the MOT results from the two-dimensional magnetic gradients: $(0, 5, -5) \text{ G/cm}$. To maximize the loading of atoms into the dipole beam, the optical tweezers are superimposed on the MOT along its long axis. In addition, we favorize the selection of atoms in the hyperfine low level $5S_{1/2}, F=1$ by removing the repump light in the overlapping region similarly to the dark MOT technique [16].

The dipole trapping beam is turned on at a power of 80 W during the 500 ms loading time of the MOT. Then, we increase the MOT detuning in 5 ms from -3Γ to -7.7Γ , Γ being the natural frequency width of the excited state. This procedure improves significantly the optical tweezers loading efficiency. Then, the magnetic field and repumping light are switched off to optically depump atoms to the $F=1$ ground sublevel. Finally all the remaining MOT beams are turned off. The number of atoms in the optical tweezers is as high as 3×10^7 , corresponding to a peak atomic density of $5 \times 10^{12} \text{ at/cm}^3$. These numbers are measured 50 ms after switching off the MOT beams, so a first evaporation has already occurred on this time scale since the collision rate is larger than 500 s^{-1} .

In order to transport a cloud in the non-adiabatic regime without spilling atoms, one has to maximize the parameter

$\eta = U_0/k_B T$ which is the ratio between the potential well depth U_0 and the average potential energy $k_B T$. We proceed in two steps. First, we cool down the sample by forced evaporation by lowering the beam power P . During this whole phase η remains roughly constant. Second, we adiabatically re-compress the trap by increasing the beam power P . In this process, U_0 scales as P and the temperature T scales as $P^{1/2}$, and thus the dimensionless parameter η increases as $P^{1/2}$. This way we can control the value of η for a given power P after compression.

Two different atom cloud preparation schemes were used. In the first one, referred to scheme 1, the initial trapping beam power is lowered in two linear ramps by a factor of 23 within 600 ms. The atomic cloud temperature before re-compression is $27 \pm 1.0 \mu\text{K}$. In scheme 2 the beam power is decreased in four linear ramps by a factor of 170 within 3300 ms, resulting in a $3.7 \pm 0.5 \mu\text{K}$ temperature of the atomic packet. The trapping beam power after compression and before transporting the atoms reaches 37 W (respectively, 42 W), and the temperature of the transported packets is $160 \pm 11 \mu\text{K}$ (respectively, $43 \pm 2 \mu\text{K}$) for scheme 1 (respectively, 2). The η parameter is thus equal to 13 for scheme 1 and 50 for scheme 2. The initial number of atoms before the transport is 2.1×10^6 (respectively, 5.7×10^6) for scheme 1 (respectively, 2).

The radial angular frequencies of the recompressed trap were inferred from a parametric heating experiment, and are on the order of 2 kHz for both schemes. The longitudinal angular frequency was measured by examining the cloud dipole mode oscillations. We find $\omega_0 = 2\pi \times (8.1 \pm 0.3) \text{ Hz}$ (respectively, $\omega_0 = 2\pi \times (8.9 \pm 0.3) \text{ Hz}$) for the scheme 1 (respectively, 2).

The transport experiment has been carried out in a single vacuum chamber. We consequently imposed a “round trip” displacement to the optical tweezers, going from the MOT location A to a point B placed at $d = 22.5 \text{ mm}$ from it along the beam direction, and back to A (see fig. 2a). The velocity of the trap as a function of time is deliberately chosen as a succession of constant acceleration for the sake of simplicity. First, the trap is accelerated at a constant rate a during a time $T/4$, decelerated at the opposite rate $-a$ during $T/2$, and finally re-accelerated at a to stop after a total transport time T . This simple velocity profile will allow us to exhibit the main features of non-adiabatic transport, and hence does not restrict the generality of the conclusions that we will draw from our experiments. The distance of transport $2d$ is simply related to the acceleration a and the transport duration T by $2d = aT^2/8$. In practice, the different transport durations that have been used were obtained by varying the acceleration a from 0.2 to 3.3 ms^{-2} , in order to investigate the non-adiabatic regime.

The transport is accompanied by a moderate heating of the cloud (on the order of $40 \mu\text{K}$ for both schemes) and no detectable atom loss as soon as the transport duration is longer than two periods of oscillation. For shorter

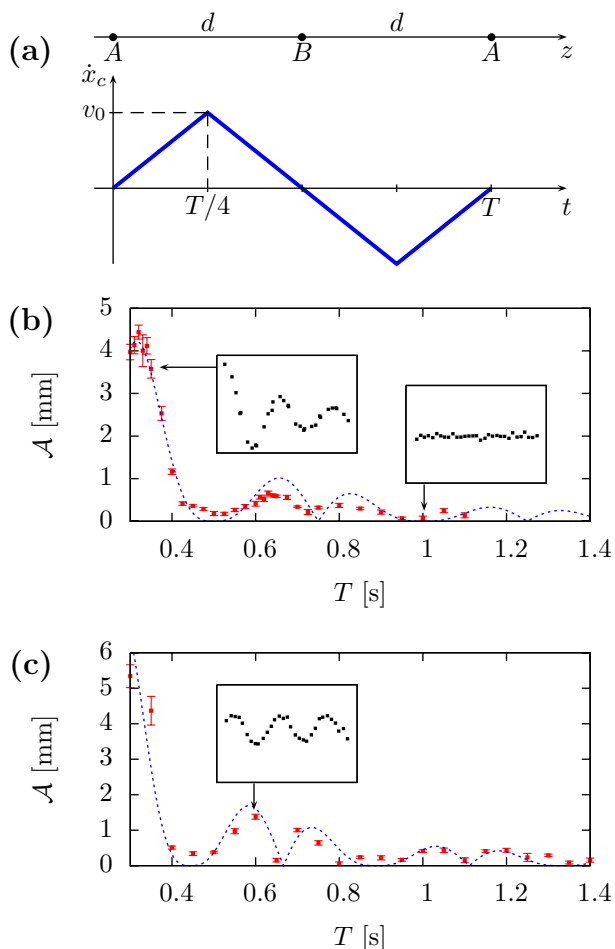


Fig. 2: (Colour on-line) (a) Velocity profile imposed to the trap to do the back and forth transport between A and B separated by $d = 22.5$ mm. (b) (respectively, (c)) The measured amplitude \mathcal{A} of the centre-of-mass dipole oscillation for the conditions of scheme 1 (respectively, 2), see text. The dashed line is the theoretical prediction of eq. (4) with the measured angular frequency ω_0 of the trap.

times the acceleration is sufficient to spill atoms out of the tweezers when $\eta = 13$. The increase of temperature is attributed to the transverse shaking of the cloud that occurs during the transport. To circumvent this limitation, we plan to use for future experiments an air-bearing translation stage instead of the standard linear rail-guided translation stage we are currently using. Note that the photon scattering rate remains relatively small for both schemes (we evaluate the photon-scattering-induced heating rate to be $3 \mu\text{K/s}$).

To infer the residual amplitude of oscillation \mathcal{A} (see fig. 2b and c), we measure the centre-of-mass oscillations after the transport by recording a set of typically 30 images separated from one another by 10 ms after the transport. The images are acquired using a standard absorption imaging technique on a CCD camera. Since the imaging process is destructive, the whole experimental sequence has to be redone for each picture. The position of the

centre of mass of the cloud as a function of time is inferred from a 2D Gaussian fit. We deduce the amplitude of oscillation by fitting the first period of this position data (see inset of fig. 2b) with a sine function.

For both schemes the variation of the amplitude as a function of the transport duration is non-monotonic. There are specific discrete transport durations for which the measured amplitude of oscillation is zero within our error bars (see second inset of fig. 2b). This shows our ability to move a packet of atoms in the non-adiabatic regime (*i.e.* in a time on the order of a few oscillation periods) with no excitation of the dipole mode of oscillation *after* the transport. Note that the dipole mode of oscillation is excited during the transport process since the transport is non-adiabatic. We point out that after such an optimal transport over a macroscopic distance, the number of atoms and temperature of the remaining cloud are compatible with the evaporative cooling to degeneracy in a crossed dipole trap geometry. Indeed we have been able to achieve Bose-Einstein condensation with such clouds by crossing vertically a $200 \mu\text{m}$ waist beam with our tweezers and ramping down both powers.

To interpret our data a simple one-dimensional analytical model is sufficient and provides a good quantitative understanding of the physics of the centre-of-mass motion of a packet of atoms transported by a moving harmonic potential. A similar formalism has been developed to transport ions in segmented Paul trap arrays [17]. We consider an atomic packet initially at rest in a harmonic trap of angular frequency ω_0 . The trap position is given by the position of its centre $x_c(t)$. As mentioned earlier, the movement of the centre of mass is decoupled from the other degrees of freedom and hence can be treated as a single particle in the harmonic trap. For a particle of mass m , the imposed motion of the trap can be considered as an extra force whose expression is $-m\ddot{x}_c(t)$ in the frame attached to the trap. According to Newton's law, the time-dependent position $x(t)$ of the centre of mass obeys the relation

$$x(t) = x_c(t) + \frac{1}{\omega_0} \int_0^t dt' \sin[\omega_0(t' - t)] \ddot{x}_c(t'). \quad (1)$$

The amplitude \mathcal{A} of the oscillatory motion after transport is readily inferred from eq. (1), and corresponds to the Fourier transform of the velocity profile of the trap's centre position

$$\mathcal{A} = |\mathcal{F}[\dot{x}_c](\omega_0)|, \quad (2)$$

with $\mathcal{F}[f] = \int_{-\infty}^{+\infty} f(t) e^{-i\omega t} dt$.

In the case of a one-way transport over a distance $d = aT^2/4$ of duration T with the simple velocity profile shown in fig. 3a (solid line), the final amplitude of oscillation is plotted in fig. 3b (solid line) and reads

$$\mathcal{A} = d \text{sinc}^2(\omega_0 T/4) \quad (3)$$

where the $\text{sinc}(x)$ function is defined as $\sin(x)/x$. It exhibits a series of discrete optimal transport durations

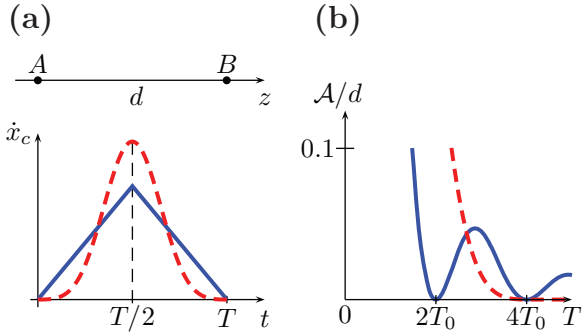


Fig. 3: (Colour on-line). (a) Two different velocity profiles to go from a point A to a point B separated by a distance d : the triangular profile (solid line) and the 4-term Blackman-Harris profile [18] (dashed line). (b) The residual amplitude \mathcal{A} of oscillation of the centre of mass after transport for these velocity profiles (see text). An optimal transport ($\mathcal{A}=0$) can be performed in two periods of oscillation in the triangle case, and in any time greater than $4T_0$ in the Blackman case.

$T_n = 2nT_0$, where $T_0 = 2\pi/\omega_0$ is the period of oscillation of the trap, and n a non-zero integer, for which the amplitude after the transport vanishes. They correspond to a transport without residual dipole mode excitation. We find, for this specific example, that it is possible to move optimally a packet of atoms on any distance d on a time as short as twice the oscillation period. This is to be contrasted with the transport in the adiabatic limit ($\omega_0 T \gg 1$) for which the transport's duration is long compared to $T_0 = 2\pi/\omega_0$. We emphasize that these optimal strategies are robust against experimental uncertainties: indeed an error of 10% on the transport duration $2T_0$ would lead to a residual amplitude of oscillation less than the one obtained when transporting ten times slower in a non-optimal manner (in $21T_0$).

In the case of a “round trip”, the amplitude of oscillation after a transport of duration T reads

$$\mathcal{A} = 2d \operatorname{sinc}^2(\omega_0 T/8) |\sin(\omega_0 T/4)|. \quad (4)$$

As expected, we find optimal transport duration corresponding to a cloud stopped after the forward motion $A \rightarrow B$. Indeed the backward motion $B \rightarrow A$ is then optimal too, and we recover the sinc^2 factor obtained for the one-way transport. In addition we obtain another set of zeros (due to the $|\sin|$ factor) for which the cloud is not at rest after the forward move. In this case, the energy given to the cloud in the first half of the motion is removed during the second part due to the time symmetry of the trajectory around $T/2$.

The dashed line in fig. 2a is given by eq. (4) rescaled by a factor of 0.6 and is in good agreement with our experimental data. The measured amplitude of oscillation is smaller than the predicted one because in our experiments the oscillation of the centre of mass is damped when its amplitude is large (see first inset of fig. 2b).

This is due to the fact that the cloud explores a potential region far away from the minimum where non-linearities play an increasing role. In this instance, particles have different periods of oscillation depending on their energy, and the observed damping results from the average taken over this spectrum of oscillation frequencies involved in a transport experiment. It means that, strictly speaking, it is impossible to transport in an optimal manner a packet of atoms in the non-adiabatic regime as soon as the potential exhibits non-linearities.

Two strategies can be used to avoid this effect. First, a longer transport time whilst remaining in the non-adiabatic regime minimizes this problem, because the cloud then remains close to the harmonic bottom of the trap. For scheme 1, we indeed observe that the damping is negligible for longer transport duration.

Alternatively, one can use a larger η parameter. The involved spectrum of oscillation frequency is then narrower, resulting in partial damping suppression. This is exemplified by the data of scheme 2 represented in fig. 2c for which $\eta=50$ (to be compared to $\eta=13$ for scheme 1), where the dashed line represents the theoretical prediction of eq. (4) without any adjustment on the amplitude. For this sufficiently large η , we recover the expected contrast of the amplitude curve (see figs. 2b and c). The simple theoretical framework that we have developed is then in very good agreement with our data.

The occurrence of optimal transport durations is a general feature of the transport in the non-adiabatic regime with a harmonic trap. They can be adjusted at will by choosing a proper velocity profile for the displacement of the trap. The duration of an optimal transport can in principle be reduced to very short time in comparison to the period of oscillation. However for practical reasons, including the finite depth of the trapping potential, there is always a limit on the acceleration one can use and thus on the minimum transportation time.

The Fourier-transform formulation (eq. (2)) of the transport allows for many enlightening analogies. For instance, the modulus square of the amplitude \mathcal{A}^2 is mathematically identical to the intensity profile for the far-field Fraunhofer diffraction pattern of an object with a transmittance having the same shape as the velocity profile for the transport. An optimal transport condition is equivalent to a dark fringe in the corresponding diffraction pattern. The “round trip” $A \rightarrow B \rightarrow A$ (see fig. 2a) considered in our experiment is made of two triangular velocity profiles corresponding to a one-way transport $A \rightarrow B$ and another in the opposite direction $B \rightarrow A$. In optics, we know that the repetition of a pattern in the transmittance yields interferences. We can thus re-interpret formula (4) where the factor term $\operatorname{sinc}^2(\omega_0 T/8)$ plays the role of a diffraction pattern for a one way transport, and the factor term $|\sin(\omega_0 T/4)|$ accounts for “interferences” between the two one-way velocity profiles. The optimization of the conditions under which a non-adiabatic transport

should be carried out with a “harmonic” optical tweezers is then equivalent to apodization problems in optics, which is a thoroughly studied problem [19]. We further emphasize that the finite width of the spectrum of periods of oscillation due to non-linearities involved in a non-adiabatic transport is reminiscent of the finite temporal coherence of the illuminating source in an optical diffraction experiment. In the case of transport the width of this spectrum depends on the duration of the transport. In optics the spectrum width is an intrinsic property of the illuminating source and therefore affects globally the whole diffraction pattern.

Another interesting analogy based on the Fourier transform formulation lies in the minimization of side lobes of the spectrum when choosing a window to perform spectral analysis, or when choosing the time shape of a Raman pulse [18,20]. For instance, the use of a 4-term Blackman-Harris shape for the velocity profile¹ should ensure a robust optimal transport as soon as its duration is bigger than $4T_0$ (see fig. 3, dashed lines), yielding a very robust optimal transport.

In conclusion, we have demonstrated the implementation of an optimal transport with optical tweezers in the non-adiabatic regime along with a simple theoretical formalism. The results presented in this letter are of interest not only for cold atoms experiments to increase their repeating rate, but also to any experiment where transport using harmonic traps is achievable like, for instance, trapped-ions experiments.

We thank J. DALIBARD and T. LAHAYE for careful reading of the manuscript. Support for this research came from the Délégation Générale pour l’Armement (DGA, contract No. 05-251487), the Institut Francilien de Recherche sur les Atomes Froids (IFRAF) and the Plan-Pluri Formation (PPF) devoted to the manipulation of cold atoms by powerful lasers. GR acknowledges support from the DGA.

¹ $\dot{x}_c(t) = 0.35875 - 0.48829 \cos(2\pi t/T) + 0.14128 \cos(4\pi t/T) - 0.01168 \cos(6\pi t/T)$.

REFERENCES

- [1] SAUER J. A., FORTIER K. M., CHANG M. S., HAMLEY C. D. and CHAPMAN M. S., *Phys. Rev. A*, **69** (2004) 051804.
- [2] COLOMBE Y., STEINMETZ T., DUBOIS G., LINKE F., HUNGER D. and REICHEL J., *Nature*, **450** (2007) 272.
- [3] GUSTAVSON T. L., CHIKKATUR A. P., LEANHARDT A. E., GÖRLITZ A., GUPTA S., PRITCHARD D. E. and KETTERLE W., *Phys. Rev. Lett.*, **88** (2001) 020401.
- [4] CHIKKATUR A. P., SHIN Y., LEANHARDT A. E., KIELPINSKI D., TSUKATA E., GUSTAVSON T. L., PRITCHARD D. E. and KETTERLE W., *Science*, **296** (2002) 2193.
- [5] LAHAYE T., REINAUDI G., WANG Z., COUVERT A. and GUÉRY-ODELIN D., *Phys. Rev. A*, **74** (2006) 033622.
- [6] LEWANDOWSKI H., HARBER D., WHITAKER D. and CORNELL E., *J. Low Temp. Phys.*, **132** (2003) 309.
- [7] NAKAGAWA K., SUZUKI Y., HORIKOSHI M. and KIM J., *Appl. Phys. B*, **81** (2005) 791.
- [8] GREINER M., BLOCH I., HÄNSCH T. W. and ESSLINGER T., *Phys. Rev. A*, **63** (2001) 031401.
- [9] HÄNSEL W., REICHEL J., HOMMELHOFF P. and HÄNSCH T. W., *Phys. Rev. Lett.*, **86** (2001) 608.
- [10] HOMMELHOFF P., HAENSEL W., STEINMETZ T., HAENSCH T. and REICHEL J., *New J. Phys.*, **7** (2005) 3.
- [11] GÜNTHER A., KEMMLER M., KRAFT S., VALE C. J., ZIMMERMANN C. and FORTÁGH J., *Phys. Rev. A*, **71** (2005) 063619.
- [12] KUHR S., ALT W., SCHRADER D., MÜLLER M., GOMER V. and MESCHEDÉ D., *Science*, **293** (2001) 278.
- [13] SCHMID S., THALHAMMER G., WINKLER K., LANG F. and DENSCHLAG J., *New J. Phys.*, **8** (2006) 159.
- [14] SCHULZ S., POSCHINGER U., SINGER K. and SCHMIDT-KALER F., *Fortschr. Phys.*, **54** (2006) 648.
- [15] GRIMM R., WEIDEMÜLLER M. and OVCHINNIKOV Y. B., *Adv. At. Mol. Opt. Phys.*, **42** (2000) 95.
- [16] KETTERLE W., DAVIS K. B., JOFFE M. A., MARTIN A. and PRITCHARD D. E., *Phys. Rev. Lett.*, **70** (1993) 2253.
- [17] REICHEL R., LEIBFRIED D., BLAKESTAD R., BRITTON J., JOST J., KNILL E., LANGER C., OZERI R., SEIDELIN S. and WINELAND D., *Fortschr. Phys.*, **54** (2006) 666.
- [18] HARRIS F., *Proc. IEEE*, **66** (1978) 51.
- [19] JACQUINOT P. and ROIZEN-DOSSIER B., *Prog. Opt.*, **3** (1964) 31.
- [20] KASEVICH M. and CHU S., *Phys. Rev. Lett.*, **69** (1992) 1741.